Chemoresponsive assemblies of microparticles at liquid crystalline interfaces

Gary M. Koenig, Jr., I-Hsin Lin, and Nicholas L. Abbott[1]

Department of Chemical and Biological Engineering, University of Wisconsin–Madison, 1415 Engineering Drive, Madison, WI 53706

Edited by Tom C. Lubensky, University of Pennsylvania, Philadelphia, PA, and approved December 23, 2009 (received for review October 1, 2009)

Assemblies formed by solid particles at interfaces have been widely studied because they serve as models of molecular phenomena, including molecular self-assembly. Solid particles adsorbed at interfaces also provide a means of stabilizing liquid–liquid emulsions and synthesizing materials with tunable mechanical, optical, or electronic properties. Whereas many past studies have investigated colloids at interfaces of isotropic liquids, recently, new types of intercolloidal interactions have been unmasked at interfaces of liquid crystals (LCs): The long-range ordering of the LCs, as well as defects within the LCs, mediates intercolloidal interactions with symmetries that differ from those observed with isotropic liquids. Herein, we report the decoration of interfaces formed between aqueous phases and nematic LCs with prescribed densities of solid, micrometer-sized particles. The microparticles assemble into chains with controlled interparticle spacing, consistent with the dipolar symmetry of the defects observed to form about each microparticle. Addition of a molecular surfactant to the aqueous phase results in a continuous ordering transition in the LC, which triggers reorganization of the microparticles, first by increasing the spacing between microparticles within chains and ultimately by forming two-dimensional arrays with local hexagonal symmetry. The ordering transition of the microparticles is reversible and is driven by surfactant-induced changes in the symmetry of the topological defects induced by the microparticles. These results demonstrate that the orderings of solid microparticles and molecular adsorbates are strongly coupled at the interfaces of LCs and that LCs offer the basis of methods for reversible, chemosensitive control of the interfacial organization of solid microparticles.

colloidal interactions | interfacial assemblies | liquid crystals | ordering transitions

A liquid crystal (LC) is a phase of matter that blends properties that are typically associated with either crystalline solids or isotropic liquids (1). The molecules that comprise nematic LC phases exhibit long-range orientational order, yet they also possess mobilities characteristic of an isotropic liquid. LCs are most widely known for their use in electrooptic displays; however, they are increasingly being studied in the context of biology, materials science, and analytical chemistry (1). Recently, for example, microdroplets and microparticles dispersed in bulk LCs have been shown to form ordered assemblies, demonstrating that LCs can provide routes to stabilizing emulsions and assembling solid particles into colloidal crystals (2, 3). Although the origins of the interparticle forces that direct the formation of these assemblies in bulk LCs are not yet completely understood, it is clear that the long-range orientational ordering of molecules within the LC phase gives rise to interparticle forces that can be described in terms of the elasticity of the LCs and formation of topological defects within the LC. The LC-mediated interparticle interactions can also be very strong, with energies of $\sim 10^3 k_B T$/particle (2, 3). In this paper, we move beyond the study of self-assembly in bulk LCs to report on the ways in which LCs can be used to direct interfacial assembly processes involving colloidal and molecular adsorbates. In particular, we focus on interfaces formed between aqueous phases and immiscible nematic LC phases and the influence of molecular adsorbates (surfactants) added to the aqueous phase on the interfacial ordering of colloids.

Interfacial environments created by two immiscible isotropic liquids, when decorated with microparticles, are known to lead to a range of interparticle forces that act parallel to the interfaces, including capillary, dipolar electrostatic, and elastic forces (4). When one of the isotropic liquids is replaced by a LC, it has recently become evident that additional mechanisms of interparticle interactions are realized. For example, glycerol microdroplets formed by condensation at a nematic LC–air interface have been reported to spontaneously self-assemble into two-dimensional assemblies with hexagonal symmetry (5–8). In this paper, we report on the reversible ordering of solid microparticles, with chemically functionalized surfaces, at LC–aqueous interfaces. In contrast to droplets, solid microparticles do not deform or coalesce in the presence of attractive interactions, and their surfaces can be chemically modified to control the interactions between the microparticle surfaces and the LC. We also focus on interfaces formed between LCs and aqueous phases because the aqueous phase enables delivery of water-soluble adsorbates (e.g., molecular surfactants) that can be used to manipulate the orientational ordering of the LC at the interface. As shown by the results of our study, LC ordering transitions induced by adsorbates can lead to reversible ordering transitions in colloidal assemblies formed at these interfaces [we note that our previous study of microparticles at LC–water interfaces employed microparticles that underwent irreversible aggregation at these interfaces (9)—*SI Text* has additional discussion of our previous experiments]. Finally, we comment that assemblies formed by solid microparticles offer the basis of a range of materials with potentially useful and tunable optical, mechanical, and electrical properties.

Results and Discussion

The goal of our first experiment was to establish a general and versatile method that would permit decoration of LC–aqueous interfaces with prescribed densities of solid microparticles. The LC used in our study was 4-pentyl-4′cyanobiphenyl (5CB), a thermotropic LC that forms a nematic LC between 24 and 35 °C (10). We used silica microparticles (diameters of 2.3 μm) functionalized with the silane dimethyloctadecyl[3-(trimethoxysilyl) propyl]ammonium chloride (DMOAP; Acros). Particles functionalized with DMOAP cause 5CB to assume a perpendicular orientation at the particle surface (2), and the covalent attachment of the DMOAP to the particle surface ensures that desorption of DMOAP from the particle surface (and potentially onto the LC–aqueous interface) does not take place (9, 11).

Author contributions: G.M.K., I.-H.L., and N.L.A. designed research; G.M.K. and I.-H.L. performed research; G.M.K., I.-H.L., and N.L.A. analyzed data; and G.M.K. and N.L.A. wrote the paper.

The authors declare no conflict of interest.

This article is a PNAS Direct Submission.

Freely available online through the PNAS open access option.

See Commentary on page 3945.

[1]To whom correspondence should be addressed. E-mail: abbott@engr.wisc.edu.

This article contains supporting information online at www.pnas.org/cgi/content/full/0910931107/DCSupplemental.

www.pnas.org/cgi/doi/10.1073/pnas.0910931107

We found that sedimentation of the DMOAP-functionalized microparticles from the aqueous phase provided the basis of a simple method to deposit the microparticles onto the nematic 5CB–aqueous interface (Fig. 1*A*). Although the microparticles were hydrophobic, with sonication and stirring, the microparticles could be singly dispersed in water and then introduced as a droplet (diameter of ~5 mm) into an aqueous phase overlying a 20-μm-thick film of nematic 5CB supported within a metal specimen grid on top of an octyltrichlorosilane (OTS) functionalized glass microscope slide (11). The individual sections of the metal specimen grid measured 280×280 μm^2, which was large compared to the size of the microparticles but small compared to the size of the droplet used to deliver the microparticles into the aqueous phase overlying the grid (the latter condition ensures that relatively uniform densities of microparticles were deposited within each grid). Individual microparticles were observed by optical microscopy to sediment through the aqueous phase and deposit at the 5CB–aqueous interface. Deposition of microparticles at the 5CB–aqueous interface coincided with a change in the optical appearance of the LC because the microparticles deposited at the interface changed the local ordering of the LC in the vicinity of each microparticle (see below for details).

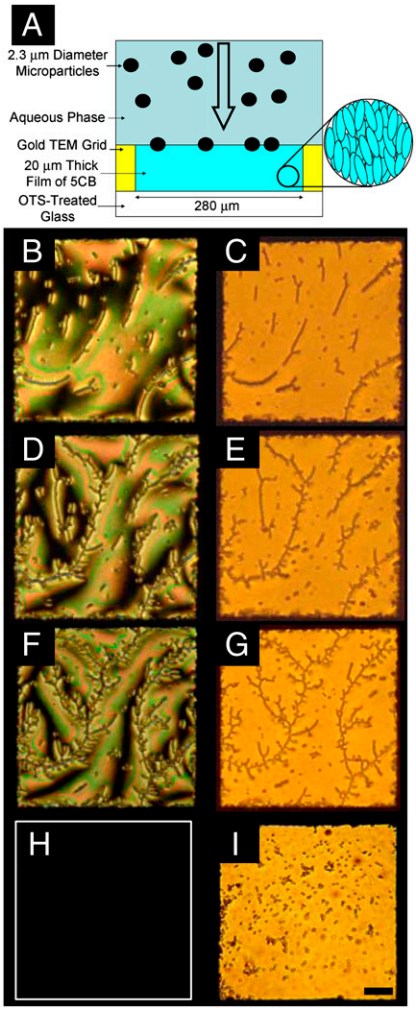

Fig. 1. (*A*) Cartoon depicting the use of sedimentation to deposit microparticles at interfaces between nematic 5CB and aqueous phases. Polarized (*B*, *D*, and *F*) and bright-field (*C*, *E*, and *G*) optical micrographs of interfacial assemblies of microparticles with areal densities of 4,500 (*B* and *C*), 9,900 (*D* and *E*), and 14, 800 microparticles/mm^2 (*F* and *G*). Polarized (*H*) and bright-field (*I*) optical micrographs of the same microparticles sedimented onto a 5CB–aqueous interface heated to 40 °C (above the nematic-to-isotropic transition temperature of 5CB). A false white border has been added to indicate in the edge of the sample (*H*). The microparticles in (*I*) appear larger than the microparticles in the other images because of a slight tilting of the sample in (*I*). (Scale bar: 50 μm.)

Fig. 1*B* and *C* are optical images (polarized light and bright-field, respectively) showing that microparticles deposited by sedimentation do collect at the 5CB–aqueous interface (surface concentration of 4, 500 microparticles/mm^2). Subsequent depositions of microparticles were performed at the same interface, resulting in surface concentrations of 9,900 (Fig. 1*D* and *E*) and 14, 800 microparticles/mm^2 (Fig. 1*F* and *G*). When preparing the interfaces shown in Fig. 1, we measured the rate of deposition of microparticles to be ~100 microparticles/mm^2 sec. The microparticles used in this study did not sediment through the 5CB–aqueous interface but, rather, were located at the interface (see *SI Text* for details) (12).

Inspection of Fig. 1*B* and *C* reveals that microparticles deposited at the LC–aqueous interface spontaneously self-assemble into chain-like structures, consistent with the presence of interparticle interactions with dipolar symmetry (i.e., chaining of dipoles) (2, 3, 13). As the density of microparticles was increased at the interface, the chains exhibited branching, and a dendritic organization became evident (Fig. 1*D*–*G*). The observation of branching is also consistent with the presence of dipolar interactions between microparticles, with branch points corresponding to pairs of microparticles with antiparallel dipoles (13). Close inspection of the polarized light micrographs in Fig. 1 also reveals that the chains of microparticles generally follow the azimuthal orientation of the LC at the aqueous interface. We elaborate on this observation later in the paper (see below).

To determine if the chaining and branching of microparticles evident in Fig. 1 was directed by the nematic ordering of 5CB, we next sedimented microparticles onto a 5CB–aqueous interface heated above the bulk nematic-to-isotropic transition temperature of 5CB (35 °C). Under these conditions, the microparticles deposited at the 5CB–aqueous interface did not form chain-like assemblies (Fig. 1*H* and *I*). Instead, the microparticles formed compact aggregates comprised of small clusters of microparticles. This result leads us to conclude that the nematic order of the 5CB is responsible for mediating interparticle interactions that lead to the chaining and branching of microparticles observed in Fig. 1.

To provide further insight into the origin of the LC-mediated interparticle interactions that lead to the chaining of microparticles evident in Fig. 1, we characterized the ordering of 5CB around isolated microparticles deposited at the 5CB–aqueous interface. Past studies have demonstrated that nematic 5CB adopts an orientation at a flat interface to water that is parallel to the interface (so-called planar anchoring of the LC; Fig. 2*A*) (11). When an isolated microparticle was observed at this interface (crossed polars, with one polarizer aligned parallel to the far-field orientation of the LC; Fig. 2*B*), bright lobes were evident around each microparticle. These lobes correspond to regions of the LC where the LC deviates in its azimuthal orientation from the far-field orientation because of the presence of the microparticle. When the same microparticle was observed by using bright-field optical microscopy (Fig. 2*C*), the scattering of light from a point defect [which can be classified as a so-called "boojum"; see *SI Text*] located to the left of the microparticle was clearly evident. Profiles of the orientation of the 5CB in the vicinity of the microparticle that are consistent with these optical micrographs are shown in Fig. 2*D* (side view) and Fig. 2*E* (top view). The dipolar symmetry of the LC orientational profile (and the associated point defect) leads to interparticle interactions at the interface that result in the chaining of microparticles at the interface (2, 3). Related observations involving microparticles dispersed in bulk LCs have also reported dipolar interactions, with a point defect giving rise to short-ranged repulsive interactions between the microparticles (2, 3). The presence of a short-range repulsive interaction is consistent with

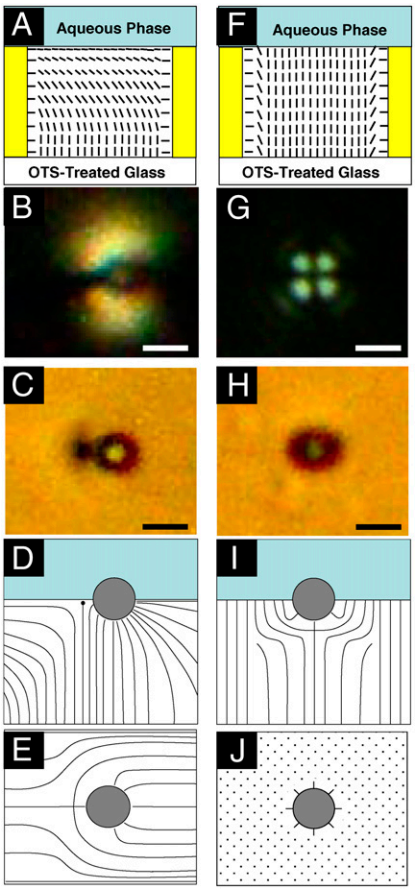

Fig. 2. (*A* and *F*) Schematic illustrations of nematic 5CB confined within a specimen grid supported on OTS-treated glass surfaces. The orientation of the nematic 5CB at the interface to the aqueous phase is shown to be parallel to the interface in (*A*, planar anchoring) and perpendicular to the interface in (*F*). Polarized (*B*) and bright-field (*C*) micrographs of a DMOAP-treated microparticle at the 5CB–aqueous interface when the ordering of 5CB at the aqueous interface was planar. Illustrations of the side view (*D*) and top view (*E*) of the LC orientation surrounding a single DMOAP-treated microparticle when the orientation of 5CB at the 5CB–aqueous interface was planar. (*G*) Polarized and (*H*) bright-field micrographs of a DMOAP-treated microparticle at the 5CB–aqueous interface when the ordering of 5CB at the aqueous interface was induced to be perpendicular by the presence of 1,300 μM SDS in the aqueous phase. Illustrations of the side view (*I*) and top view (*J*) of the orientational profile of the LC around an isolated DMOAP-treated microparticle when the orientation of 5CB at the 5CB–aqueous interface is perpendicular. (Scale bars: 2 μm.)

our observation of a well-defined spacing between microparticles within the interfacial chains of microparticles (see below for detailed discussion).

Past studies have shown that surfactants added to aqueous phases in contact with nematic 5CB will adsorb at the 5CB–aqueous interface and trigger a concentration-dependent continuous ordering transition in the 5CB. At high surfactant concentrations, the 5CB assumes an orientation at the 5CB–aqueous interface that is perpendicular to the interface (so-called homeotropic anchoring; Fig. 2*F*) (11). We sought to determine the influence of such surfactant-induced LC ordering transitions on the ordering of 5CB near microparticles located at the 5CB–aqueous interface. In our initial experiment, the anionic surfactant SDS was added to the aqueous phase to a final concentration of 1,300 μM, which is above the threshold concentration required to change the orientation of the 5CB at the 5CB–aqueous interface from planar to homeotropic (11). Inspection of the polarized (Fig. 2*G*) and bright-field (Fig. 2*H*) optical micrographs of an isolated microparticle at the 5CB–aqueous interface after addition of surfactant shows that the symmetry of the ordering of the LC in the vicinity of the microparticle has been changed by the introduction of the surfactant. In particular, the point defect in the LC is no longer visible in the bright-field image (Fig. 2*H*), and a cross-like optical signature is evident in the polarized light micrograph (Fig. 2*G*). These micrographs of LC near isolated microparticles at surfactant-decorated 5CB–aqueous interfaces are consistent with the profiles of the LC shown in Fig. 2*I* and *J*. In these profiles, it is evident that, relative to the profile of the LC observed in the absence of SDS, the point defect has relocated to a position that is directly below the particle at the interface. That is, during the adsorption of the SDS, the defect relocates to below the microparticle, thus corresponding to a surfactant-induced rotation of the topological dipole by 90°.

Because the chaining of microparticles shown in Fig. 1 was concluded to be because of LC-mediated interactions associated with the chaining of topological dipoles oriented in the plane of the interface (Fig. 2*D*), we hypothesized that the rotation of the topological dipoles induced by adsorption of SDS at the 5CB–aqueous interface (Fig. 2*I*) would lead to reorganization of the microparticle chains. Here we note that the energy of a pair of microparticles interacting through LC-mediated forces with dipolar symmetry can be estimated as $U = 4\pi KCa^4 (1 - 3\cos^2(\theta))/R^3$, where K is the elastic constant of the LC (10^{-11} N for 5CB), C is a constant [estimated to be ~25 from theory (14) and ~6 from experimental measurements (15)], a is the radius of the microparticle, θ is the angle of the dipole of one microparticle with respect to a second microparticle, and R is the separation between the microparticles. Because θ is 0° for planar ordering of LC at the 5CB–aqueous interface (Fig. 2*D*) and 90° for perpendicular ordering of 5CB at the 5CB–aqueous interface (Fig. 2*I*), this expression predicts that rotation of the topological dipole of the LC by the SDS (Fig. 2*D–I*) should change the LC-mediated dipolar interaction between the microparticles from attractive to repulsive.

To investigate the impact of interfacial adsorption of SDS on the ordering of microparticles at the LC–aqueous interface, a concentrated solution of SDS was mixed into an aqueous phase overlying a microparticle-decorated 5CB–aqueous interface. Inspection of regions of the 5CB–aqueous interface that were far from the microparticles confirmed that the LC at the interface underwent a continuous orientational transition from a planar orientation at low concentrations of SDS to a homeotropic orientation at high SDS concentrations, as evidenced by continuous changes in the interference colors seen in polarized light micrographs (Fig. 3*C*, *E*, and *G*). At concentrations of SDS above 1,000 μM, the LC at the interface adopted the homeotropic orientation (Figs. 2*F* and 3*I*), which resulted in a dark optical appearance between crossed polars. Concurrent with the SDS-induced LC ordering transition at the aqueous interface, we observed the assemblies of microparticles to undergo a change in organization. Whereas SDS concentrations below 550 μM (Fig. 3*A–D*) did not measurably perturb the microparticle spacing within the chains, we measured the spacing between nearest-neighbor microparticles within each chain to increase with SDS concentration at SDS concentrations between 550 and 950 μM (Fig. 3*E–H*). When the SDS concentration was increased from 950 (Fig. 3*G* and *H*) to 1,300 μM (Fig. 3*I* and *J*), the microparticles transformed abruptly in their organization from the chain-like structure into a two-dimensional assembly with regions that exhibited local hexagonal symmetry (discussed in more detail below).

We observed the above-described transition in the microparticle organization from branched chains to two-dimensional arrays to be reversible and to coincide with the concentration-dependent adsorption and desorption of SDS from the aqueous phase (Fig. 4 and Fig. S1) (11). We note, in addition, that the transformation of the microparticle ordering into the two-

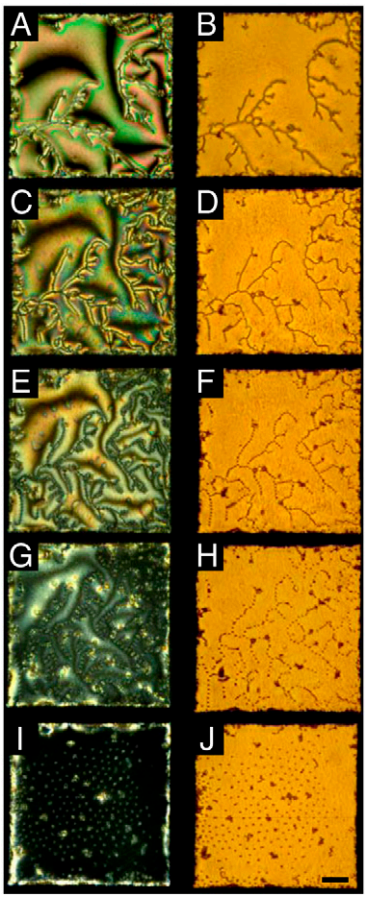

Fig. 3. Optical micrographs of SDS-induced reordering of microparticle assemblies formed at the nematic 5CB–aqueous interface. The concentrations of SDS in the aqueous phase were 150 (*A* and *B*), 550 (*C* and *D*), 700 (*E* and *F*), 950 (*G* and *H*), and 1,300 μM (*I* and *J*). Images in the left column were obtained with crossed polars, and images in the right column were obtained in bright-field imaging conditions. (Scale bar: 50 μm.)

dimensional assembly did not result in uniform coverage of the microparticles over the interface, but instead we observed regions of the interface that were depleted of microparticles (Fig. 3*I* and *J*). The observation of coexistence of particle-rich and particle-depleted regions suggests that the interactions between the particles in the two-dimensional assembly are not purely repulsive, but that a long-range attractive interaction must also be generated between microparticles at these interfaces (discussed in further detail below). We also comment on the existence of a subpopulation of compact, irreversibly associated aggregates at the 5CB–aqueous interface. These aggregates were not generated during the surfactant-induced ordering transitions of the microparticles but rather were observed to form during sedimentation of the microparticles onto the 5CB–aqueous interface.

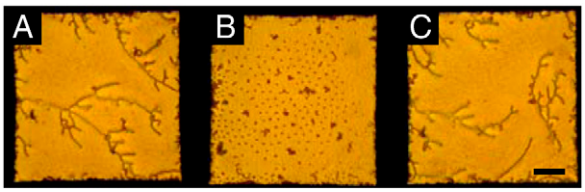

Fig. 4. Bright-field optical micrographs demonstrating the reversible ordering transition of microparticles assembled at a nematic 5CB–aqueous interface upon the adsorption and desorption of the surfactant SDS. The concentration of SDS in the aqueous phase was <5 (*A* and *C*) and 1,300 μM (*B*). Additional images can be found in Fig. S1. (Scale bar: 50 μm.)

Additional micrographs of microparticle assemblies formed at the 5CB–aqueous interface in the presence of SDS (400 and 1,100 μM) can be found in Fig. S2. By heating the 5CB above the bulk nematic-to-isotropic phase transition (to 40 °C), we also confirmed that nematic ordering of 5CB was necessary in order to form the hexagonal arrays of the microparticles (with SDS concentration of 1,300 μM): Upon heating of the 5CB into the isotropic phase, the microparticles were observed to lose their hexagonal order and form small dense aggregates on the interface (Fig. S3).

As noted above, at intermediate concentrations of SDS, we observed the microparticles to maintain their chain-like organization but exhibit SDS-dependent nearest-neighbor spacings within the chains. For microparticles and microdroplets dispersed in bulk LCs, the equilibrium spacing between the centers of colloids with dipolar defects has been experimentally determined to be ~2.6*a* (3), where *a* is the radius of the microparticle or microdroplet. For the microparticles used in this study, that separation would correspond to ~3 μm. In the absence of SDS, by analyzing bright-field micrographs, we determined the nearest-neighbor spacing of microparticles within chains at the 5CB–aqueous interface to be 3.2 ± 0.4 μm. The standard deviation in this measurement reflects the variation in the spacing between microparticles (for a population of at least 500 microparticles) and not the error in measurement of the microparticle spacing (that error was <50 nm). The close agreement between the microparticle separation observed in bulk 5CB and at the 5CB–aqueous interface is consistent with our conclusion that the dipolar topological defects formed about the interfacial microparticles (in the absence of SDS) are approximately parallel to the 5CB–aqueous interface.

Fig. 5*A* quantifies the nearest-neighbor interparticle spacing within the chains of microparticles as a function of SDS concentration. Consistent with the qualitative observations noted above regarding Fig. 3, the center-to-center nearest-neighbor separation increases from 3.2 ± 0.4 μm in the absence of SDS to 7.5 ± 0.8 μm in the presence of 950 μM of SDS. These interparticle spacings were determined to be highly reproducible as a function of SDS concentration, and they were invariant when the experimental systems were equilibrated for more than an hour (Fig. 5*B*; see Fig. S4 for corresponding optical micrographs). These results indicate that the interparticle spacings within the chains are not defined by dynamic phenomena associated with the process of SDS adsorption, but rather they are a function of the equilibrium SDS-induced ordering of the 5CB at the aqueous interface. The SDS-dependent increase in spacing of the microparticles within the chains is consistent with a decrease in the long-ranged attractive interactions between microparticles as the topological dipoles accompanying each microparticle are rotated at the 5CB–aqueous interface. In brief, the interparticle separation reflects a balance between a short-ranged repulsion associated with the point defect (which is responsible for the finite separation maintained between the surfaces of the microparticles in the absence of SDS) (2, 3) and a long-ranged attraction associated with the strain of the LC. A decrease in the strength of the long-ranged attractive interaction because of rotation of the topological dipole will thus result in an increase in the interparticle separation.

As noted above, at an SDS concentration between 950 and 1,300 μM, we observed the microparticles to undergo an ordering transition from the chain-like assemblies to two-dimensional arrays. The formation of the two-dimensional array was observed in regions of the interface that were free of the compact aggregates formed upon deposition of the microparticles onto the interface (see above). In those regions that were free of compact aggregates, we analyzed the ordering of microparticles (Fig. 5*C*) by using Voronoi tessellations (16). In a Voronoi tessellation, each microparticle is represented as a polygon, and the number of sides of the polygon is defined by the number of nearest neighbors for that microparticle. In Fig. 5*A*, a green hexagon has been

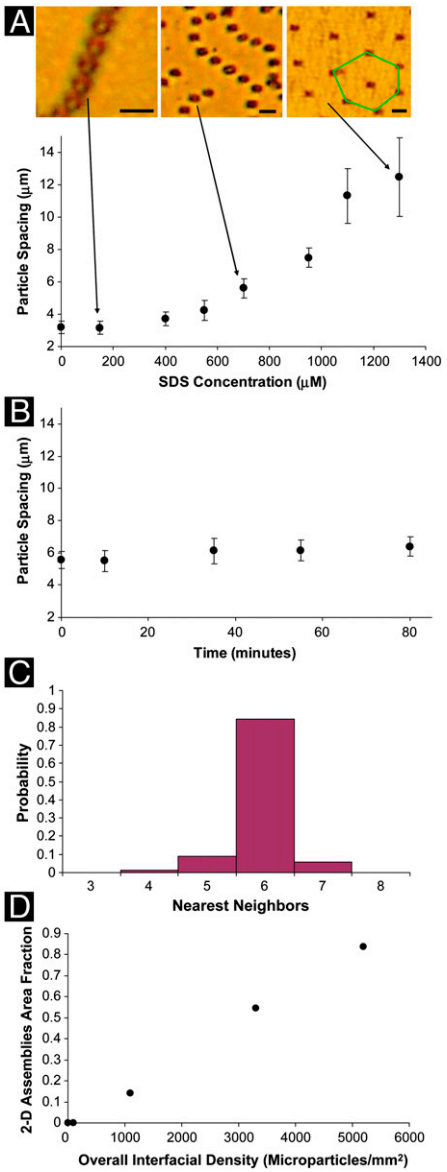

Fig. 5. (*A*) Center-to-center, nearest-neighbor spacing of microparticles within chains of microparticles formed at the LC–aqueous interface, plotted as a function of the concentration of SDS in the aqueous phase. Images are bright-field micrographs of microparticles at the nematic 5CB–aqueous interface with aqueous phase SDS concentrations of 150, 700, and 1,300 μM. (Scale bars: 5 μm.) (*B*) Center-to-center, nearest-neighbor spacing of microparticles, measured as a function of time, for microparticles assembled at the 5CB–aqueous interface in the presence of 700 μM SDS in the aqueous phase. (*C*) Probability of finding a given number of nearest neighbors for microparticles in regions free of compact aggregates when the SDS concentration in the aqueous phase was 1,300 μM. (*D*) Increase in the area fraction of the 5CB–aqueous interface (SDS concentration of 1,300 μM) occupied by regions of 2D microparticle assemblies with hexagonal symmetry, plotted as a function of the overall concentration of microparticles at the interface.

added to highlight a microparticle within an area of the interface that possesses hexagonal symmetry (six nearest neighbors). On the basis of an analysis of 600 microparticles taken from more than 10 different samples, we determined that the probability of finding six nearest neighbors was 84.1% (Fig. 5*C*), confirming the qualitative observation of hexagonal symmetry in the presence of 1,300 μM of SDS.

Assemblies of microparticles formed at interfaces of isotropic liquids have been reported previously to undergo transitions from chain-like structures to two-dimensional arrays when external fields have been applied to the interface (17, 18). In particular, assemblies of magnetic microparticles at a glycerin–air interface (17) and polystyrene microparticles dispersed in a thin film of magnetic fluid (18) have been shown to undergo an ordering transition when an applied magnetic field is rotated from parallel to normal to the interface/thin film. In those studies, the rotation of the external field led to rotation of an induced magnetic dipole and thus an abrupt transition between chains and a two-dimensional array (17). In our experiments, the adsorption of SDS leads to rotation of the topological dipole in the nematic 5CB about the microparticles at the interface and thus results in an ordering transition of the microparticles. Although the similarity between the field-induced and adsorbate-induced transitions in microparticle organization is striking, we also note some important differences. For example, the above-described studies of field-induced ordering transitions have not reported changes in nearest-neighbor spacing of microparticles within the chains prior to the transition to the two-dimensional array, as is observed in our experiments. These observations and others suggest that the analogy between these systems is only partial. In particular, short-ranged repulsions between microparticles, which are generated by the point defects in the LC systems (Fig. 2*D*), are absent in the above-described experiments involving magnetic fields.

As noted above in the context of Fig. 3*J*, the SDS-induced ordering transition that results in the two-dimensional array of microparticles is also accompanied by the formation of regions at the 5CB–aqueous interface that are devoid of microparticles. This observation is surprising because the interactions between microparticles due to topological dipoles oriented perpendicular to the surface should be purely repulsive. To gain further insight into these attractive interactions, we performed experiments in which we varied the density of microparticles deposited at the 5CB–aqueous interface and then induced the ordering transition in the microparticles by addition of 1,300 μM of SDS (see micrographs in Fig. S5). In these experiments, we observed microparticles to form two-dimensional assemblies with hexagonal symmetry for microparticle densities between 1,100 and 5,200 microparticles/mm^2. As the density of microparticles at the interface decreased, the area fraction of the interface that was devoid of microparticles was observed to increase (Fig. 5*D*). In addition, within the regions of the interface occupied by the arrays of microparticles, the nearest-neighbor center-to-center spacing of the microparticles did not change (within the standard deviation of the measurements). For very low densities of microparticles deposited at the 5CB–aqueous interface (100 microparticles/mm^2), we did not observe assemblies with hexagonal symmetry to form upon addition of SDS. These results suggest that the interfacial concentration of microparticles needs to be above a threshold value in order to form the two-dimensional packing. Above that threshold concentration, coexistence of particle-dense (hexagonal arrays) and particle-void areas is observed. These observations hint that the cohesive interactions between microparticles, which lead to the coexistence of microparticle-rich and microparticle-lean regions of the interface in the presence of SDS, may be collective, as discussed in more detail below.

Past studies of the interactions of microdroplets confined at the interface of a LC have also found evidence of attractive interdroplet interactions (4–7, 19–23). The attractive forces were initially attributed to a many-bodied "elastic–capillary" interaction between microdroplets (5, 7, 19, 20). More recently, however, the role of the elastic–capillary interaction has been questioned (4, 22, 23), and the attraction that stabilizes arrays of microdroplets has been proposed to be because of "genuine many-body effects" (22) and a universal collective attraction of clusters of microdroplets at interfaces that provides enhancement of up to 10^5 compared to pairwise attractions (23). Our observation that micro-

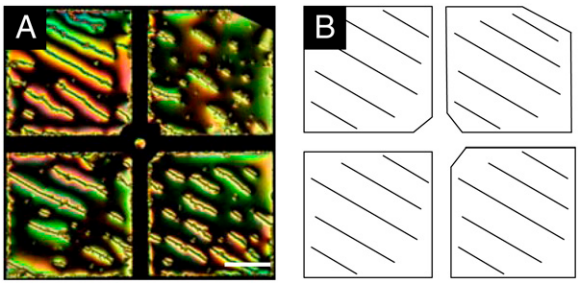

Fig. 6. (*A*) Polarized optical micrograph of microparticle chains at the nematic 5CB–aqueous interface when the azimuthal ordering of the 5CB at the interface was controlled by patterning the underlying substrate. (*B*) Cartoon depicting the azimuthal alignment of the LC. (Scale bar: 100 μm.)

particles at 5CB–aqueous interfaces form two-dimensional arrays stabilized by an attractive force (and correspondingly, regions void of particles), when combined with our observation of the absence of hexagonal arrays at low particle densities, is consistent with the presence of some type of many-bodied attractive interaction between the microparticles at this interface. Our understanding of the origin of these interactions, however, is not complete and will be the subject of future studies.

As noted above, we interpreted the results shown in Fig. 1 to suggest that chains of microparticles formed at the 5CB–aqueous interface (no SDS) follow the azimuthal ordering of the nematic 5CB. Whereas the azimuthal orientation of the 5CB was not controlled in the experiment performed in Fig. 1, we sought to determine if the orientations of chains of microparticles could be defined by supporting the 5CB on a chemical template that oriented the LC (see *SI Text* for experimental details) (24). We used an underlying substrate that was treated to provide uniform planar alignment of the 5CB. Fig. 6*A* is a polarized light micrograph of chains of microparticles at the 5CB–aqueous interface supported above one of these substrates that provided uniform planar ordering in the bulk of the thin film of 5CB. The orientation of the LC is shown in Fig. 6*B*. Inspection of Fig. 6 reveals that the orientation of long chains of microparticles can indeed be directed through control of the azimuthal orientation of the LC. This simple result provides further evidence that the forces between the microparticles were dipolar in nature and that they were directed by the azimuthal orientation of the 5CB at the 5CB–aqueous interface (for an additional micrograph, see Fig. S6). The result also demonstrates that the microparticles form chains at the LC–aqueous interface, independent of whether the LC film is anchoring perpendicular (Fig. 1) or parallel (Fig. 6) to the bottom substrate.

In conclusion, we have demonstrated that microparticle assemblies formed at a LC–aqueous interface can be driven through changes in symmetry (from chains to two-dimensional arrays) via adsorbate-induced ordering transitions in the LC. The ordering of the microparticles was reversible and clearly established to be because of interparticle interactions that are mediated by the order of the LC. We conclude that LCs provide routes to the dynamic control of ordering transitions of microparticles at fluid–fluid interfaces without the use of an external applied field. The possibility of using interfacial nematic fields present within LCs to direct the ordering of microparticle assemblies may enable control of reversible ordering transitions of microparticles at the interfaces of systems with complex geometries, such as at the surface of a droplet (12), which could be used for dynamic tuning of emulsion stability and interfacial rheological properties. The results presented in this paper also guide the design of interfacial assemblies of microparticles that can have tunable mechanical (25), optical (26), and electronic properties (27). For example, precise control over interparticle spacing within chains of microparticles, when combined with control of microparticle orientation, could be used to create tunable media for transport of light.

Materials and Methods

Additional information can be found in *SI Text*, which includes: time scale of the reversible cycling of the microparticle structures at the 5CB–aqueous interface; patterning the underlying substrate in contact with the 5CB; micrographs of cycling between chains and two-dimensional arrays; supplemental micrographs to Fig. 3; micrographs of two-dimensional arrays of microparticles cycled above and below the nematic-to-isotropic transition temperature of 5CB; micrographs of microparticle chains at a 5CB–aqueous interface as a function of time at a constant concentration of 700 μM SDS in the aqueous phase; micrographs of two-dimensional arrays of microparticles with increasing interfacial microparticle densities; and an additional image of microparticle chains directed by using a patterned underlying substrate.

ACKNOWLEDGMENTS. The authors thank Mr. Aaron Lowe for helpful discussions. This research was partially supported by the University of Wisconsin, Nanoscale Science and Engineering Center (DMR-0425880 and DMR-0832760).

1. Collings PJ (1990) *Liquid Crystals: Nature's Delicate Phase of Matter* (Princeton Univ Press, Princeton, NJ).
2. Musevic I, Skarabot M, Tkalec U, Ravnik M, Zumer S (2006) Two-dimensional nematic colloidal crystals self-assembled by topological defects. *Science*, 313:954–958.
3. Poulin P, Stark H, Lubensky TC, Weitz DA (1997) Novel colloidal interactions in anisotropic fluids. *Science*, 275:1770–1773.
4. Oettel M, Dietrich S (2008) Colloidal interactions at fluid interfaces. *Langmuir*, 24:1425–1441.
5. Nych AB, et al. (2007) Coexistence of two colloidal crystals at the nematic-liquid-crystal-air interface. *Phys Rev Lett*, 98:057801.
6. Nazarenko VG, Nych AB, Lev BI (2001) Crystal structure in nematic emulsion. *Phys Rev Lett*, 87:075504.
7. Smalyukh II, et al. (2004) Ordered droplet structures at the liquid crystal surface and elastic-capillary colloidal interactions. *Phys Rev Lett*, 93:117801.
8. Han J (2009) Ordered structures of glycerol droplets suspended in nematic liquid crystals. *J Korean Phys Soc*, 54(2):805–808.
9. Lin IH, Koenig GM, de Pablo JJ, Abbott NL (2008) Ordering of solid microparticles at liquid crystal-water interfaces. *J Phys Chem B*, 112:16552–16558.
10. EMD (2007) *Technical Data Sheet: LCG K15* (EMD Chemicals Inc., Hawthorne, NY).
11. Brake JM, Daschner MK, Luk Y-Y, Abbott NL (2003) Biomolecular interactions at phospholipid-decorated surfaces of liquid crystals. *Science*, 302:2094–2097.
12. Binks BP (2002) Particles as surfactants—Similarities and differences. *Curr Opin Colloid In*, 7:21–41.
13. Loudet JC, Richard H, Sigaud G, Poulin P (2000) Nonaqueous liquid crystal emulsions. *Langmuir*, 16:6724–6730.
14. Lubensky TC, Pettey D, Currier N, Stark H (1998) Topological defects and interactions in nematic emulsions. *Phys Rev E*, 57:610–625.
15. Poulin P, Cabuil V, Weitz DA (1997) Direct measurement of colloidal forces in an anisotropic solvent. *Phys Rev Lett*, 79:4862–4865.
16. Okabe A, Boots B, Sugihara K, Chiu SN (2000) *Spatial Tesselations: Concepts and Applications of Voronoi Diagrams* (Wiley, New York).
17. Wen W, Zhang L, Sheng P (2000) Planar magnetic colloidal crystals. *Phys Rev Lett*, 85:5464–5467.
18. Skjeltorp AT (1983) One- and two-dimensional crystallization of magnetic holes. *Phys Rev Lett*, 51:2306–2309.
19. Lev B, Chernyshuk SB, Yamamoto T, Yamamoto J, Yokoyama H (2008) Photochemical switching between colloidal photonic crystals at the nematic-air interface. *Phys Rev E*, 78:020701.
20. Ognysta UM, Nych AB, Nazarenko VG, Lev BI (2007) Interaction between droplets in nematic emulsion under the action of external fields. *Ukr Fiz Zh*, 52:633–638.
21. Andrienko D, Tasinkevych M, Dietrich S (2005) Effective pair interactions between colloidal particles at a nematic-isotropic interface. *Europhys Lett*, 70:95–101.
22. Oettel M, Dominguez A, Tasinkevych M, Dietrich S (2009) Effective interactions of colloids on nematic films. *Eur Phys J E*, 28:99–111.
23. Pergamenshchik VM (2009) Strong collective attraction in colloidal clusters on a liquid-air interface. *Phys Rev E*, 79:011407.
24. Gupta VK, Abbott NL (1997) Design of surfaces for patterned alignment of liquid crystals on planar and curved substrates. *Science*, 276:1533–1536.
25. Aussillous P, Quei D (2001) Liquid marbles. *Nature*, 411:924–927.
26. Kim B, Tripp SL, Wei A (2001) Tuning the optical properties of large gold nanoparticle arrays. *Mat Res Soc Symp Proc*, 676:Y61.61–Y61.67.
27. Velev OD, Kaler EW (2000) Structured porous materials via colloidal crystal templating: From inorganic oxides to metals. *Adv Mater*, 12:531–534.